

THE SHAPE OF THE SPECULAR PEAK OF ROUGH SURFACES

Gerhard Meister, André Rothkirch, Hartwig Spitzer, Johann Bienlein

Affiliation: CENSIS, II. Institute for Experimental Physics, University of Hamburg

Mail address: KOGS / CENSIS, Vogt-Kölln-Str. 30, D-22527 Hamburg, Germany

email: meister@informatik.uni-hamburg.de

KEY WORDS: Surface reflectance, urban objects, computer vision, modelling, BRDF

ABSTRACT

The BRDF model developed by Torrance and Sparrow describes the specular reflection of rough surfaces. We compared this model to BRDF measurements of 4 man-made surfaces with very different roughnesses. We found that the azimuthal width of the specular peak decreases strongly with increasing illumination zenith angle, in the data as well as in the model. We furthermore propose a simplification of the model by dropping one of the assumptions on the surface structure. This simplification is equivalent to ignoring masking and shadowing effects, but alters the resulting BRDF in most cases only negligibly, and provides several advantages like easier implementation and faster computing time.

1 INTRODUCTION

The reflection of light from rough surfaces is a subject of importance to remote sensing as well as computer vision. Smooth surfaces can be considered specular, i.e. the incident irradiance is reflected into one direction only. It is a common assumption that rough surfaces are lambertian, i.e. the incoming irradiance is reflected isotropically into every direction. However, most man-made rough surfaces show a broadened specular peak, and its effects can be either useful for information extraction or disturbing for conventional algorithms in image interpretation in case the surfaces are regarded as either perfectly specular or lambertian. This study evaluates the exact shape of the specular peak for rough surfaces, based on samples important for remote sensing of urban areas (roof tiles, concrete, etc.).

The specular reflection model of rough surfaces by Torrance and Sparrow (called TS model from here on) has received widespread attention ((Ginneken et al., 1998), (Oren and Nayar, 1995), (Dana et al., 1999), (Meister et al., 1998), (Rothkirch et al., 2000)). It has been criticized (e.g. by (Ginneken et al., 1998)) for its unrealistic assumptions about the surface structure. In this paper, we will show that the implications of the surface structure assumed by (Torrance and Sparrow (1967)) are quite negligible in most cases. This explains why the TS model is usually in good agreement with measurements despite its unrealistic surface structure. We will present a simplified model whose predictions are hardly distinguishable from the original model and define its range of application. The advantages of this simplified model are

- no need for unrealistic assumptions on the surface structure
- significantly reduced computation time
- the model is completely analytical (no 'if' clauses)
- simple implementation.

Furthermore we will demonstrate a feature of the TS model (and verify it with measured data) that has up to now not been discussed in the literature: the azimuthal width of the specular peak decreases strongly with increasing incidence zenith angle. This significant characteristic of the specular peak is yet another reason to prefer the TS model to other models such as e.g. the widely used Phong model (Lafortune and Willems., 1994).

2 TS MODEL

The specular peak of rough surfaces does not reach its maximum when the illumination zenith angle equals the reflection zenith angle (forward scattering direction), but the maximum is shifted towards higher reflection zenith angles. This behaviour can be well described by the popular BRDF model of (Torrance and Sparrow (1967)). It is given by

$$\begin{aligned} f_r^{\text{TS}} &= t_0 + t_1 \cdot f_r^{\text{spec}}, \\ f_r^{\text{spec}} &= \frac{F(\theta_i, \theta_r, \varphi, n, k)}{\cos \theta_i \cos \theta_r} \cdot G(\theta_i, \theta_r, \varphi) \cdot e^{-w^2 \alpha^2} \end{aligned} \quad (1)$$

where F is the Fresnel reflectance, a function of the index of refraction n , the coefficient of absorption k and the local illumination angle. The zenith angles of incidence and reflection are given by θ_i and θ_r , φ is the relative azimuth angle. t_0 is the Lambertian component, t_1 describes the intensity of the specular component. G is the 'Geometric Attenuation Factor', which takes on values between 0 and 1. Basically, this model assumes that the surface is made up of surface facets, whose normals α have a normal probability distribution $P(\alpha)$:

$$P(\alpha) \propto e^{-w^2\alpha^2} \quad (2)$$

so the width of the distribution is determined by w . (Torrance and Sparrow (1967)) use α with the unit 'degree', thus w has the unit degree^{-1} . According to (Ginneken et al., 1998), α can be calculated as

$$\cos \alpha = (\cos \theta_i + \cos \theta_r) \cdot ((\cos \varphi \sin \theta_r + \sin \theta_i)^2 + \sin^2 \varphi \sin^2 \theta_r + (\cos \theta_i + \cos \theta_r)^2)^{-\frac{1}{2}} \quad (3)$$

More specifically, in the TS model it is assumed that each surface facet is next to a surface facet whose surface normal has the same inclination α , but is oriented into the opposite direction (the azimuth angle of the second surface normal differs by 180 degrees from the azimuth angle of the first surface normal), forming a V-cavity. In fact, this is a very *unrealistic* assumption, because the inclinations of neighboring facets are usually *uncorrelated*. This assumption was introduced because for this kind of V-cavity, it is possible to derive the shadowing and masking effects analytically in the principal plane (relative azimuth equals 0° or 180°). These effects are expressed by the Geometric Attenuation Factor G . (Unfortunately, outside the principal plane the angles needed to determine G are calculated using several 'if' clauses, complicating the implementation severely, especially if the derivative of the TS model is needed, e.g. for least-square-fitting procedures.) We conclude that because of the unrealistic assumption of V-cavities, the usefulness of the TS model is questionable. However, as we will show later, for most surfaces the influence of G is negligible. This means that for most surfaces, masking and shadowing does not play a major role for the specular peak, and the assumption of V-cavities becomes *unnecessary*.

Furthermore it is assumed that the V-cavities are indefinitely long. This is an *unrealistic* assumption as well, in fact there is no reason why the length of a surface facet should be significantly longer than its width. However, this assumption is largely equivalent to ignoring edge effects, thus we believe that it is a *justified simplification*.

3 DATA ACQUISITION

Our data was acquired in a measurement campaign at the European Goniometric Facility (EGO) at the Joint Research Center (JRC), Ispra, Italy. EGO allows reflectance measurements with arbitrary viewing and illumination angles (Solheim et al., 1996).

The goniometer at EGO consists of two quarter arcs with a radius of 2 m (see (Rothkirch et al., 1999) or (Rothkirch et al., 2000) for illustrations). A sensor and a light source can be attached to the arcs, their position on the arc determines the zenith angle. The arcs can be moved on a circular rail (radius: 2 m), determining the azimuth angle. The angles can be positioned with an accuracy of 0.1° . Several light sources and sensors are available, we used a 1000 W halogen lamp and a spectroradiometer SE590, Spectron Engineering Inc., Denver, USA. Data were acquired in the wavelength range from 425 nm to 975 nm. The target samples were man-made surfaces typical of urban areas:

- red roof tile (baked clay)
- black roof paper covered with sand
- asphalt
- red painted aluminum
- red concrete tile
- blue concrete tile

The chosen targets are ideal for laboratory measurements because of their homogeneity and temporal invariance (opposed to e.g. vegetation samples). Furthermore we measured two reference samples (Spectralon panels with an albedo of 0.5 resp. 0.99) to convert the reflected radiances to BRDF values, see (Meister et al., 1999) for a detailed report on the data processing. The average total error depends strongly on the spectral signature of the sample, varying from 4 % to up to 15 %.

The shape of the specular peak of these 8 samples was measured while varying zenith as well as azimuth angles. Neither the reference panels nor the asphalt sample show a strong specular peak. The sample 'black roof paper covered with sand' has a strongly nonlambertian BRDF even without considering the specular peak, the diffuse BRDF rises with increasing zenith angle. But in the TS model, the diffuse component is assumed to be lambertian. Thus we will reduce our analysis to the four samples roof tile, aluminum, blue concrete and red concrete.

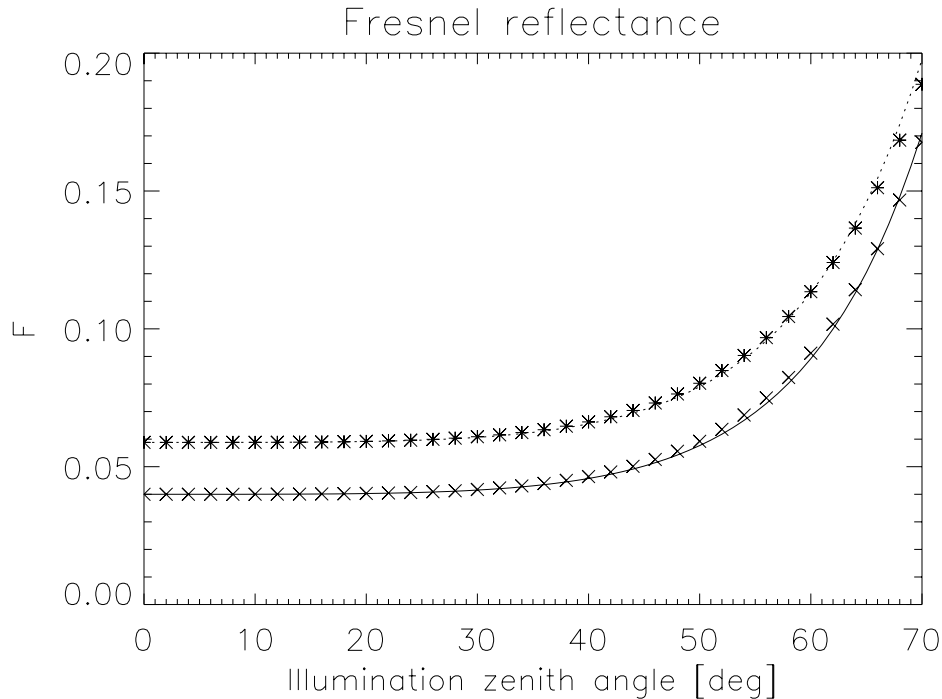


Figure 1: The Fresnel reflectance for unpolarized illumination as a function of illumination angle for different parameters n, k . The solid line shows the Fresnel reflectance for $k = 0$ and $n = 1.5$, the crosses show the Fresnel reflectance for $k = 0.4$ and $n = 1.35$, normalized to the value $\theta_i = 0^\circ$ of the solid line. The dotted line shows the Fresnel reflectance for $k = 0.2, n = 1.6$, the stars show the Fresnel reflectance for $k = 0.55, n = 1.4$, normalized to the value of the dotted line at $\theta_i = 0^\circ$

4 VALIDATION

For this study, we will restrict the analysis to a wavelength of 550 nm, because we found that at this wavelength the measurement errors are lowest (Meister et al., 1999). The same results can be obtained with any other wavelength in the measured range (425 nm to 975 nm).

We fitted the parameters of the TS model to our data using a least-square fitting routine from the programming package IDL. We did not use measurements with a relative azimuth φ smaller than 90° , because we want to focus our investigation on the specular peak. For the roof tile we obtained 145 measurements, for the other 3 samples 122 measurements. The TS model is driven by 5 parameters: t_0, t_1, w, n and k . Thus the number of measurements is clearly sufficient. But the parameters k and n cannot be retrieved simultaneously, their effect on the Fresnel reflectance in conjunction with the specular intensity parameter t_1 is not unique. This can be seen from fig. 1. The solid line shows the Fresnel reflectance for $k = 0$ and $n = 1.5$ as a function of illumination angle θ_i . The crosses show the Fresnel reflectance for $k = 0.4$ and $n = 1.35$, normalized to the value $\theta_i = 0^\circ$ of the solid line. It can be seen that different parameters k produce a very similar Fresnel reflectance if the parameters n and the specular intensity parameter t_1 are adjusted. The dotted line (Fresnel reflectance with $k = 0.2, n = 1.6$) shows another example: it can hardly be separated from the stars (Fresnel reflectance with $k = 0.55, n = 1.4$, normalized to the value of the dotted line at $\theta_i = 0^\circ$). Thus it is impossible to retrieve the parameters k, n and the specular intensity parameter from BRDF measurements if neither of them is known. Additional information can be obtained from e.g. polarized BRDF measurements (as presented in (Rothkirch et al., 2000)), which allow a much better discrimination between the parameters n and k .

Thus it sounds justifiable to set $k = 0$, like in e.g. (Ginneken et al., 1998). However, $k = 0$ is incompatible with the polarized BRDF measurements presented in (Rothkirch et al., 2000) on the same red roof tile as used in this study. We adopted the value of $k = 0.25$ from (Rothkirch et al., 2000) and set this parameter constant for all samples. The value of n we obtain from fitting (see table 1) using $k = 0.25$ is higher than the value given in (Rothkirch et al., 2000) ($n = 1.35$). Thus we conclude that the Fresnel parameters n and k retrieved by fitting can describe the shape of the specular peak very well, but probably cannot be regarded as true physical parameters. This may be due to the unrealistic modelling of masking and shadowing in the TS model.

The fitted parameters t_0, t_1, w and n are given in table 1 for the 4 samples. d_f denotes the degrees of freedom (number of

Sample	t_0 [sr ⁻¹]	t_1 [sr ⁻¹]	w [deg ⁻¹]	n	k	χ^2/d_f
Spectralon 50 %	0.157 ± 0.001	0.14 ± 0.1	0.032 ± 0.002	1.58 ± 0.9	0.25 ± 2.1	1.2
Roof tile	0.0245 ± 0.0003	0.20 ± 0.05	0.0362 ± 0.0004	1.77 ± 0.3	0.25 ± 1.1	4.1
Red concrete	0.0192 ± 0.0001	1.06 ± 0.2	0.0804 ± 0.0005	1.48 ± 0.11	0.25 ± 0.3	5.1
Blue concrete	0.0685 ± 0.0003	1.07 ± 0.2	0.0832 ± 0.0008	1.48 ± 0.16	0.25 ± 0.4	1.7
Red Aluminum	0.0101 ± 0.0001	2.99 ± 0.8	0.153 ± 0.001	1.73 ± 0.27	0.25 ± 0.9	16.7

Table 1: Parameter obtained from fitting the TS model (eq. 1) to the BRDF data of the respective sample at a wavelength of 550 nm. The parameter k was set to 0.25. See text for a discussion of the errors.

measurements (N) minus number of parameters (5 in this case)), χ^2 is defined as

$$\chi^2 = \sum_i^N \frac{(f_{r,i}^{\text{measured}} - f_{r,i}^{\text{modelled}})^2}{\sigma_i^2} \quad (4)$$

where σ_i is the measurement error of the i 'th measured BRDF value $f_{r,i}^{\text{measured}}$. The fit does not pass the χ^2 test (except for the Spectralon reference panel), but it is unclear whether this is due to the simplifying assumption of a lambertian diffuse BRDF (coefficient t_0) in the TS model or due to a failure to exactly model the specular peak. The errors were calculated according to (Brandt, 1992) using a Taylor expansion because of the nonlinearity of the fitting function. The errors can only be seen as rough estimates, because the Taylor expansion of the Fresnel reflectance

$$F(k + \sigma_k) = F(k) + \frac{\delta F}{k} \cdot \sigma_k \quad (5)$$

is a poor approximation for the large σ_k of table 1. Furthermore the parameters have to be treated with caution, because the fits do not pass the χ^2 test.

The model BRDF values are plotted in figs. 2 and 3 (solid line), together with measured values (crosses). The measurement errors are plotted as vertical bars, often they are so small that they can hardly be seen in the plot. The plots show that the model fits the measurements quite well, the strongest deviations occur for the sample red aluminum, where the intensity of the specular peak is underestimated. The BRDF values of the Spectralon 50 % panel are also shown. Although the specular peak is relatively weak, it cannot be ignored, especially for large illumination angles (see (Meister et al., 1996) or (Meister et al., 1999) for a more exact representation of the Spectralon BRDF, where the diffuse component is no longer required to be lambertian).

Fig. 2 shows the well known shift of the maximum of the specular peak towards higher zenith angles (especially for $\theta_i = 50^\circ$). The roof tile has a very broad specular peak, the aluminum has a very sharp specular peak, and the width of the specular peak of the concrete tiles is in between. The widths corresponds to facet inclination distributions (see eq. 2) with average surface normals α of 17.6°, 15.6°, 7.0°, 6.8°, 3.7° for Spectralon, roof tile, red concrete, blue concrete and red aluminum, respectively.

Fig. 3 shows a feature of the TS model that has up to now not been discussed in the literature. The BRDF values are plotted as a function of the relative azimuth angle φ , with $\theta_r = \theta_i$ for $\theta_i = 30^\circ$ and $\theta_i = 50^\circ$, and $\theta_r = 70^\circ$ for $\theta_i = 65^\circ$. It can be seen that the width of the peaks with respect to the azimuth angle decreases dramatically with increasing zenith angle. For a better comparison, the last plot in each row shows the measured values minus t_0 (i.e. the specular peak, without the diffuse component) of the three previous plots normalized to the maximum value. It can be seen that the azimuthal width reduces by about 50 % when increasing θ_i from 30° to 50°, and by about 75 % when increasing θ_i from 30° to 65°. The dramatic change of shape of the specular peak data, which is obviously in accord with the TS model, is not predicted by simpler models like e.g. the Phong model (Lafortune and Willems., 1994). Thus the TS model is clearly preferable.

The mathematical explanation for this effect can be found in eq. 3 of the TS model. Let us assume an illumination zenith angle of $\theta_i = 45^\circ$. To direct the incoming ray to either $\theta_r = 35^\circ, \varphi = 180^\circ$ or $\theta_r = 55^\circ, \varphi = 180^\circ$, i.e. a variation of 10° within the principal plane, a surface facet with normal $\alpha = 5^\circ$ is needed according to eq. 3 (oriented towards the light source for $\theta_r = 35^\circ$, oriented away from the light source at $\theta_r = 55^\circ$). This result is independent of θ_i . To direct the ray to $\theta_r = 45^\circ, \varphi = 170^\circ$, i.e. 10° out of the principal plane, we also need a surface facet with a normal of 5°. But this result depends strongly on θ_i . For $\theta_i = 65^\circ$, we need a surface facet with a normal of $\alpha = 10.6^\circ$ to direct the ray to $\theta_r = 65^\circ, \varphi = 170^\circ$. For $\theta_i = 30^\circ$, we need a surface normal of only $\alpha = 2.9^\circ$. The amount of surface facets with normal α is given by eq. 2. $\alpha = 0^\circ$ is the most abundant surface normal, the probability of a surface facet having the normal α decreases monotonously with α . In the case of $\theta_i = 65^\circ$, this means that there are more surface facets with a normal of $\alpha = 5^\circ$ (needed to direct the light towards $\theta_r = 75^\circ, \varphi = 180^\circ$) than surface facets with a normal of $\alpha = 10.6^\circ$ (needed

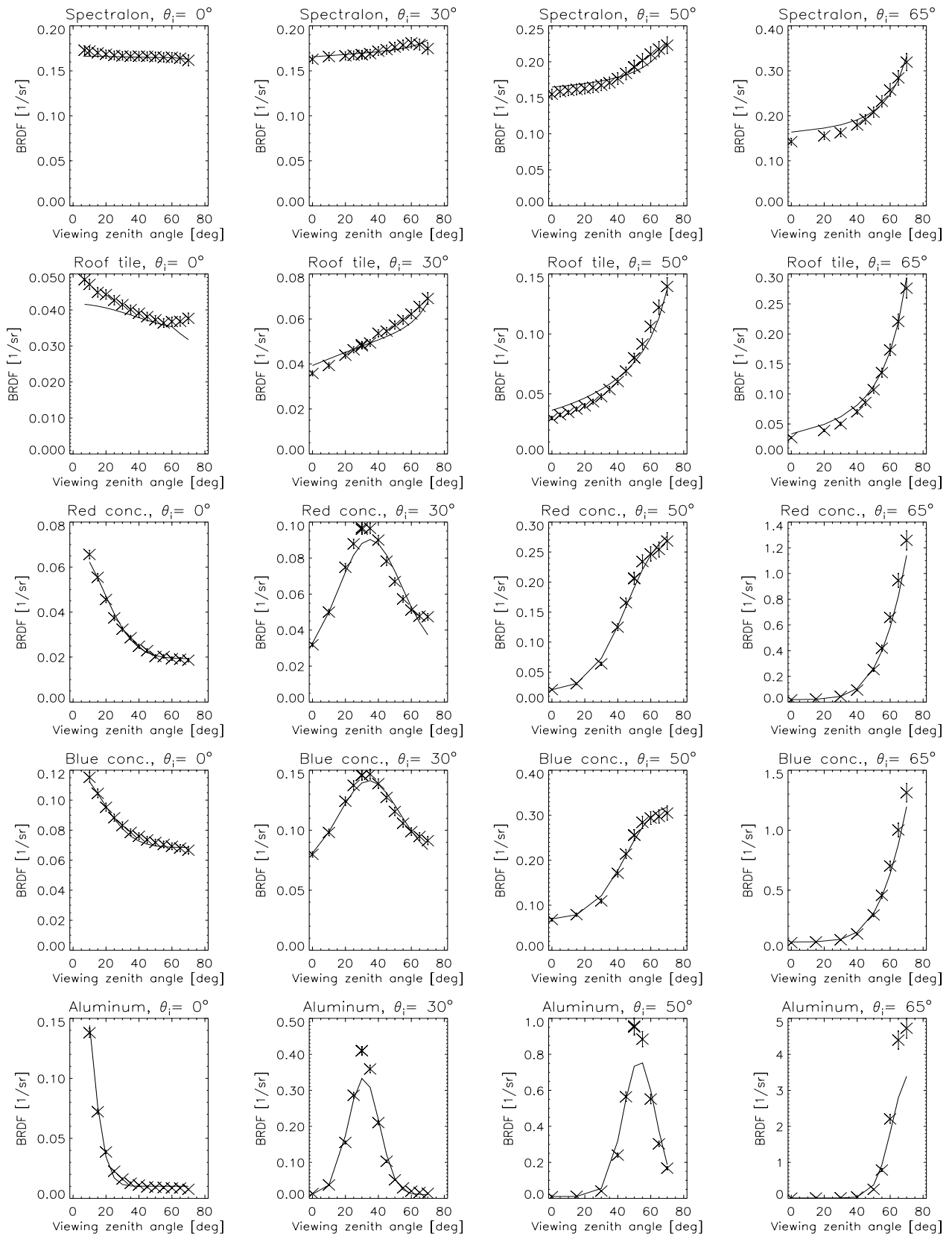


Figure 2: BRDF of the samples as a function of viewing zenith angle in forward scattering direction ($\varphi = 180^\circ$). Stars denote measured values, the solid line shows the TS model predictions using the parameters from table 1. The samples have specular peaks of different intensity and widths (widest for roof tile, narrowest for aluminum).

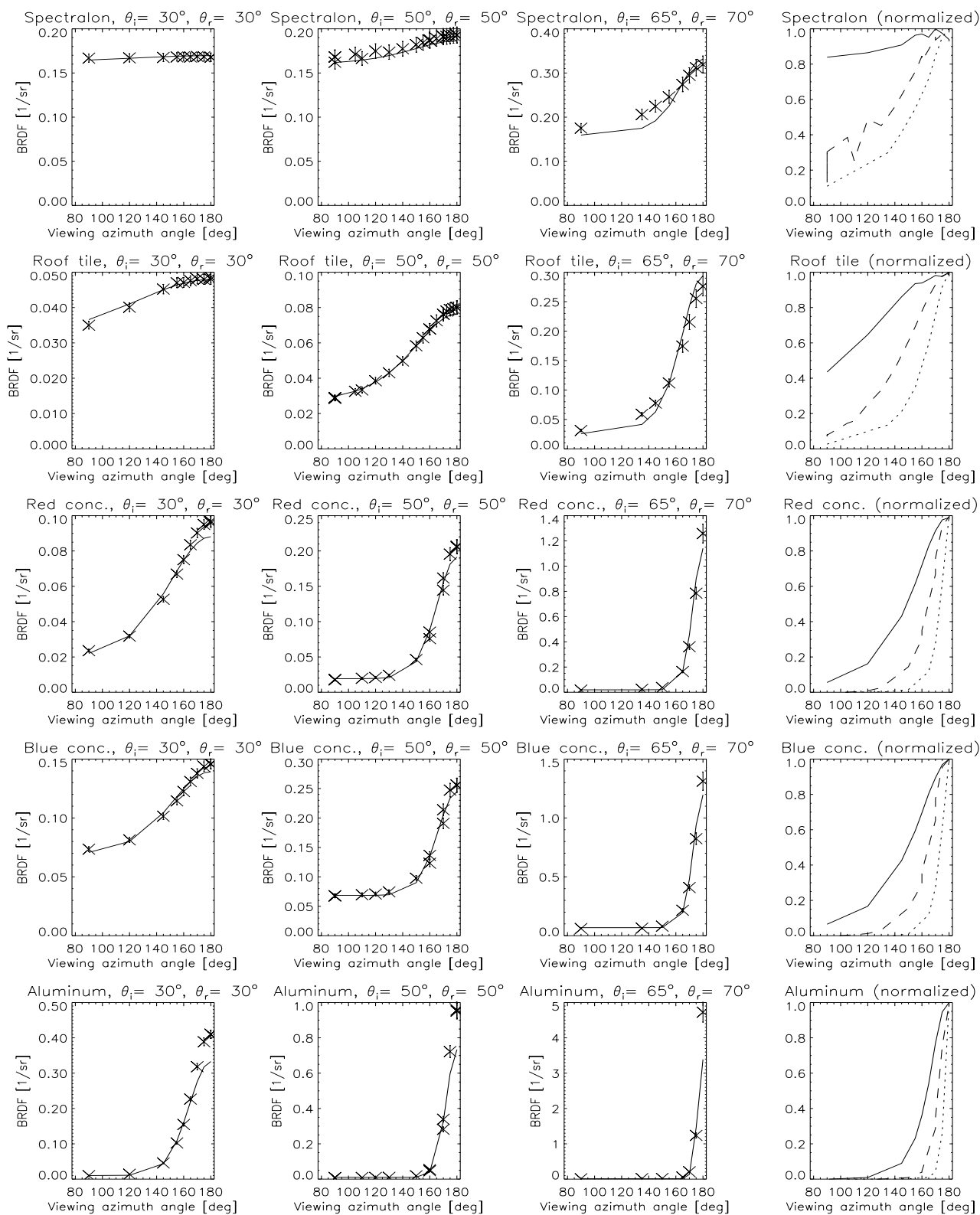


Figure 3: BRDF of the samples as a function of azimuth angle. Stars denote measured values, the solid line shows the TS model predictions using the parameters from table 1. The last column shows the measured specular peak only (i.e. the measured values minus the coefficient t_0) normalized to its maximum value. Solid line shows $\theta_i = \theta_r = 30^\circ$, dashed line shows $\theta_i = \theta_r = 50^\circ$ and dotted line shows $\theta_i = 65^\circ, \theta_r = 70^\circ$. It can be seen that the azimuthal width of the specular peak decreases strongly with increasing zenith angles.

to direct the light towards $\theta_r = 65^\circ, \varphi = 170^\circ$). Thus the intensity of reflected light is weaker at $\theta_r = 65^\circ, \varphi = 170^\circ$ than at $\theta_r = 75^\circ, \varphi = 180^\circ$, i.e. the azimuthal width of the specular peak decreases for high illumination angles.

We expected a decrease of the azimuthal width, because the azimuthal width covered by a fixed solid angle decreases with increasing zenith angle (a solid angle covering $\Delta\theta = \Delta\varphi = 1^\circ$ at $\theta = 90^\circ$ still has a zenithal width of $\Delta\theta = 1^\circ$ at nadir, but an azimuthal width of $\Delta\varphi = 180^\circ$). However, it is surprising to find that the azimuthal width even becomes smaller than the zenithal width above approximately 45° .

This effect was confirmed by a simple experiment: we directed a laser towards a tilted mirror at a high illumination angle, and turned the mirror around its axis. The light beam hit a vertical plane, and we marked the path of the light ray while turning the mirror. After projecting the vertical plane onto a sphere covering the upper hemisphere, we obtained an ellipse, the larger axis in the vertical, the smaller axis in the horizontal direction. (Note that the specular peak predicted by the TS model is not an ellipse due to the Fresnel reflectance F , the Geometric Attenuation Factor G , and most notably the division by the cosines of the zenith angles, see eq. 1.)

It is important to recognize that only the *shape* of the specular peak changes with illumination angle. The overall *intensity* of the specular peak also depends on the illumination angle, but only because of the Fresnel Reflectance F (and masking and shadowing effects). The effect of the reduction in azimuthal width on the total intensity is compensated by the division by the cosine of the illumination zenith angle $\cos\theta_i$ in eq. 1.

5 SIMPLIFIED MODEL

As explained in section 2, the assumptions of V-cavities in the TS model is highly unrealistic. In this section, we will show that in most cases it is possible to drop this assumption without changing the model predictions.

The assumption of V-cavities was introduced to derive G , the Geometric Attenuation Factor, describing shadowing and masking. G is shown in fig. 4 as a function of α , the inclination of the surface facet, for the principal plane, i.e. $\varphi = 0^\circ$ or $\varphi = 180^\circ$, and several illumination angles ($\theta_i = 0^\circ, 40^\circ, 60^\circ, 80^\circ$). It can be seen that G always equals one for $\alpha = 0^\circ$, this means at $\theta_i = \theta_r, \varphi = 180^\circ$ there is no masking or shadowing for any illumination angle predicted by the TS model (a rather questionable prediction, by the way). Let us take a closer look at the solid line, showing G for $\theta_i = 0^\circ$. G equals 1 for $|\alpha| < 30^\circ$. The angular width of the specular peak of most rough surfaces is usually much smaller. In a second measurement campaign at the JRC, Ispra, using the EGO with a different detector and measuring the BRDF in the principal plane of 20 man-made surfaces typical for urban areas, we found no specular surfaces with a broader peak than the sample 'roof tile' presented here. The width of the specular peak of the sample roof tile is given by $w = 0.035$. According to equation 2, this means that for 70 % of all surface normals $|\alpha| < 30^\circ$. This means that only 30 % of the specular peak is affected by the Geometric Attenuation Factor at all. Furthermore, the angles where $G \neq 1$ are usually quite far away from the center of the specular peak (for $\theta_i = 0^\circ, \alpha = 30^\circ$ leads to $\theta_r = 60^\circ$, cf. solid line in fig. 5), the measured intensity is usually so small that it is difficult to separate it from the diffuse component. Similar consequences apply for $\theta_i = 60^\circ$ (dotted line in fig. 4 resp. fig. 5): $G = 1$ for $\alpha = 10^\circ$, i.e. even at $\theta_r = 80^\circ$ there is no effect from masking or shadowing in the TS model. Also at $\theta_i = 60^\circ, G = 1$ for $\alpha = -30^\circ$, i.e. even at $\theta_r = 0^\circ$ there is no effect from masking or shadowing, according to the TS model.

These findings lead us to investigate what difference can be expected when neglecting shadowing and masking completely, i.e. setting $G = 1$ for all angles. We assumed a lambertian diffuse component with an albedo of 0.01, and a specular peak determined by the parameters of the specular peak of the roof tile (for samples with a more narrow specular peak or a diffuse albedo greater than 0.01 the differences are even smaller). For $\theta_i, \theta_r \leq 60^\circ, \varphi \in [0^\circ, 180^\circ]$ there is no difference at all. For $\theta_i, \theta_r \leq 65^\circ$, the maximum relative difference is 14 % (occurring at $\theta_i = 0^\circ, \theta_r = 65^\circ$, resp. $\theta_r = 65^\circ, \theta_i = 0^\circ$), the maximum absolute difference is $\Delta f_r = 0.0019 \text{ sr}^{-1}$ (or $\Delta BRDF = \pi \cdot \Delta f_r = 0.006$). For $\theta_i, \theta_r \leq 70^\circ$, the maximum relative difference is 34 %, the maximum absolute difference is $\Delta f_r = 0.0044 \text{ sr}^{-1}$ (or $\Delta BRDF = \pi \cdot \Delta f_r = 0.014$). These values can be seen as a worst-case differences (because of the wide specular peak and the low diffuse albedo). To present more representative values, we also calculated the differences for the 4 samples whose specular peak we presented above. For $\theta_i, \theta_r \leq 70^\circ, \varphi \in [0^\circ, 180^\circ]$, we obtain maximum relative differences of 10.3 %, 1.0 %, 0.3 % and $< 0.1\%$ for the samples red roof tile, red concrete tile, blue concrete tile and red painted aluminum, respectively. *Thus we conclude that for most samples, the effect of the Geometric Attenuation Factor G is negligible for zenith angles $\leq 70^\circ$.* This is simply equivalent to ignoring masking and shadowing effects predicted by the TS model.

However, in case the albedo needs to be calculated, obviously zenith angles $\geq 70^\circ$ cannot be ignored. Thus, for albedo calculation, the simplified model should *not* be used.

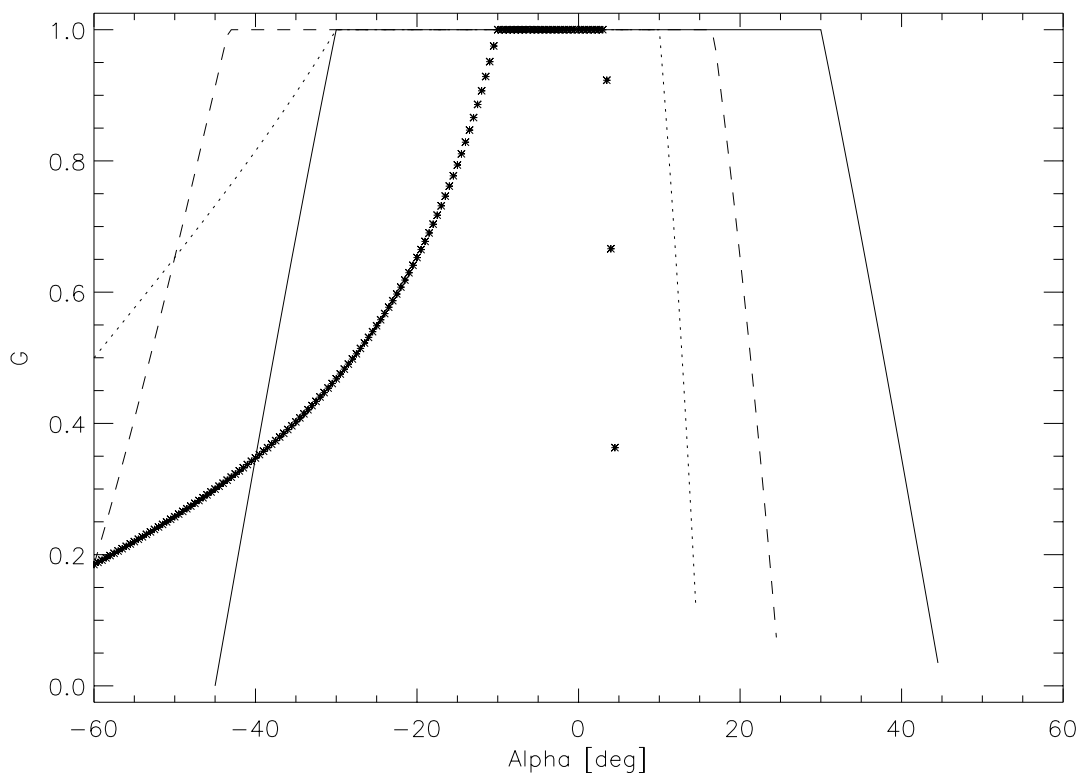


Figure 4: Geometric Attenuation Factor G as a function of the surface facet normal α for different illumination angles in the principal plane. Negative angles α correspond to a surface facet inclined towards the light source, positive α corresponds to surface facets tilted away from the light source. Solid line: $\theta_i = 0^\circ$, dashed line: $\theta_i = 40^\circ$, dotted line: $\theta_i = 60^\circ$, stars: $\theta_i = 80^\circ$.

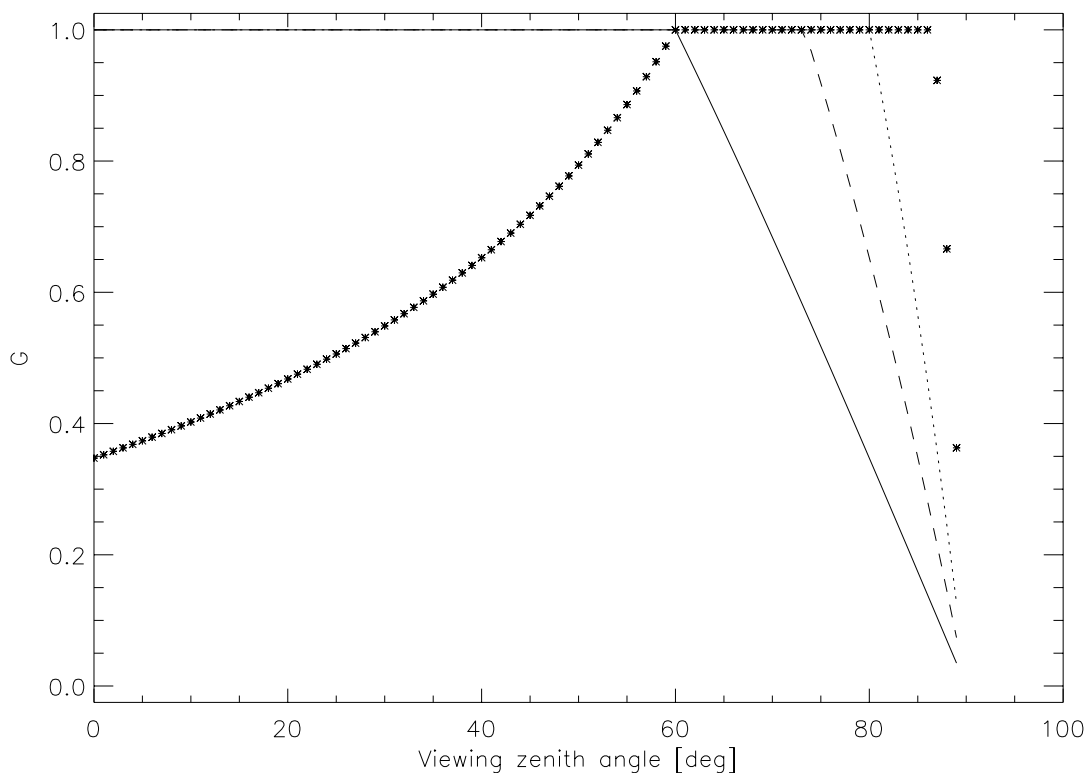


Figure 5: Geometric Attenuation Factor G as a function of the viewing zenith angle θ_r for different illumination angles. Solid line: $\theta_i = 0^\circ$, dashed line: $\theta_i = 40^\circ$, dotted line: $\theta_i = 60^\circ$, stars: $\theta_i = 80^\circ$.

6 CONCLUSIONS

The TS model was compared to BRDF measurements of 4 man-made surfaces with very different roughnesses. The shift of the maximum of the specular peak was confirmed. In this study, we furthermore found a feature of the specular peak of rough surfaces that has gone unnoticed before: the azimuthal width of the specular peak decreases strongly with increasing illumination zenith angle. For zenith angles above approximately 45° , the azimuthal width becomes smaller than the zenithal width.

The TS model is based on the assumption of V-shaped cavities. We propose a simplification of the model by dropping this assumption. This is equivalent to ignoring masking and shadowing effects, but alters the resulting BRDF in most cases only negligibly for zenith angles up to 70° , especially for surfaces with a narrow specular peak or a strong diffuse albedo.

Acknowledgements

We thank Brian Hosgood, Giovanni Andreoli and Alois Sieber from JRC, Ispra for their support in acquiring the BRDF data with the EGO goniometer.

REFERENCES

- S. Brandt, 1992. *Datenanalyse*, BI-Wissenschaftsverlag, Mannheim, Leipzig, Wien, Zürich, pp. 276
- K.J. Dana, B.v. Ginneken, S.K. Nayar and J.J. Koenderink, 1999. Reflectance and Texture of Real World Surfaces, ACM Transactions on Graphics, Vol. 18, no. 1, pp. 1-34
- B.v. Ginneken, M. Stavridi and J.J. Koenderink, 1998. Diffuse and specular reflectance from rough surfaces, Applied Optics, Vol. 37, no. 1, pp. 130-139
- B. Hapke, 1993. Theory of Reflectance and Emittance Spectroscopy, Cambridge University Press, Cambridge
- M. Oren and S.K. Nayar, 1995. Generalization of the Lambertian Model and Implications for Machine Vision, International Journal of Computer Vision, Vol. 14, pp. 227-251
- G. Meister, R. Wiemker, J. Bienlein and H. Spitzer, 1996. In Situ BRDF Measurements of Selected Surface Materials to Improve Analysis of Remotely Sensed Multispectral Imagery, Vol. XXXI part B7, Proceedings of ISPRS 1996, Vienna, pp. 493-498
- G. Meister, R. Wiemker, R. Monno, H. Spitzer and A. Strahler, 1998. Investigation on the Torrance-Sparrow Specular BRDF Model, Proceedings of IGARSS'98, Seattle, IEEE, Vol. IV, pp. 2095-2097
- G. Meister, A. Rothkirch, B. Hosgood, H. Spitzer and J. Bienlein, 1999. Error Analysis for BRDF Measurements at the European Goniometric Facility, Remote Sensing Reviews, submitted
- G. Meister, A. Rothkirch, J. Bienlein and H. Spitzer, 1999. BRDF Studies for Remote Sensing of Urban Areas, Remote Sensing Reviews (submitted)
- E.P. Lafortune and Y.D. Willems, 1994. Using the Modified Phong Reflectance Model for Physically based Rendering, Report CW 197, Nov 1994, Department of computing Science, K.U. Leuven
- A. Rothkirch, G. Meister, B. Hosgood, H. Spitzer and J. Bienlein, 1999. BRDF Measurements at the EGO using a Laser Source: Equipment characteristics and estimation of error sources, Remote Sensing Reviews, submitted
- A. Rothkirch, G. Meister, H. Spitzer and J. Bienlein, 2000. BRDF Measurements of Urban Surface Materials at the EGO Facility Using a Laser Source, Proceedings of ISPRS 2000, Amsterdam, this issue
- S. Solheim, B. Hosgood, G. Andreoli and J. Piironen, 1996. Calibration and Characterization of Data from the European Goniometric Facility (EGO), Report EUR 17268 EN, SAI, JRC, Ispra, Italy
- K. Torrance and E. Sparrow, 1967. Theory for Off-Specular Reflection from Rough Surfaces, Journal of the Optical Society of America, Vol. 57, pp. 1105-1114.